Electronic Supplementary Information for

Synergistically Optimizing the Optoelectronic Properties and Morphology via Photo-Active Solid Additive for High-Performance Binary Organic Photovoltaics

Mengting Wang,[a] Tianyi Chen,[a] Yaokai Li,[a] Guanyu Ding,[a] Zeng Chen,[c] Jikun Li,[h] Chang Xu,[a] Wupur Adiljan,[a] Chenran Xu,[d] Yuang Fu,[e] Jingwei Xue,[f] Weifei Fu,[b] Weiming Qiu,[i] Xi Yang,[i] Dawei Wang,[d] Wei Ma,[f] Xinhui Lu,[e] Haiming Zhu,[c] Xiankai Chen,[g] Xiaoye Wang,[h] Hongzheng Chen[a,b] and Lijian Zuo*[a,b]*

[a] State Key Laboratory of Silicon and Advanced Semiconductor Materials, Department of Polymer Science and Engineering, Zhejiang University, Hangzhou 310027, P. R. China.

E-mail: hzchen@zju.edu.cn ; zjuzlj@zju.edu.cn

[b] Zhejiang University-Hangzhou Global Scientific and Technological Innovation Center, Hangzhou 310014, P. R. China.

[c] Department of Chemistry, Zhejiang University, Hangzhou 310027, P. R. China.

[d] Zhejiang Province Key Laboratory of Quantum Technology and Device, School of Physics, and State Key Laboratory for Extreme Photonics and Instrumentation, Zhejiang University, Hangzhou 310027, P.R. China.

[e] Department of Physics, The Chinese University of Hong Kong, New Territories, Hong Kong 999077, P. R. China.

[f] State Key Laboratory for Mechanical Behavior of Materials Xi'an Jiaotong University, Xi'an Jiaotong University, Xi'an 710049, P. R. China.

[g] Institute of Functional Nano and Soft Materials, Joint International Research Laboratory of Carbon-Based Functional Materials and Devices, Soochow University, Suzhou 215123, P. R. China.

[h] State Key Laboratory of Element-Organic Chemistry, College of Chemistry, Nankai University, Tianjin 300071, P.R. China.

[i] Guangzhou Chasinglight Technology Co., Ltd

Supplementary Experimental Procedures

Materials

The PM6, BTP-eC9, and PDINN were purchased from Organtec Ltd. The 4CzIPN were purchased from Aladdin Inc. The BNH were synthesized by co-worker Xiaoye Wang, and has already reported before. PEDOT:PSS was purchased from Heraeus Company Limited.

Small-area Device Fabrication

Organic photovoltaics were fabricated on glass substrates pre-coated with a layer of indium tin oxide (ITO) with the structure of ITO/PEDOT:PSS/Active layer/PDINN/Ag. Before fabrication, the substrates were subjected to a series of cleaning agents including detergent, deionized water, acetone, and isopropanol, with each step lasting for 10-20 minutes. Subsequently, the pre-treated ITO substrates were exposed to an ultraviolet ozone generator for a duration of 20 minutes, followed by being spin-coating of PEDOT:PSS (Clevios^{TM} 4083) at 4000 rpm. After baking the PEDOT:PSS layer in air at 150℃ for 15 min, the substrates were transferred into the N_2 glovebox to ensure a controlled environment. For all blends, the total concentration was maintained at 16.2 mg·ml^{-1} dissolved in chloroform, with a fixed donor-acceptor (D:A) weight ratio of 1:1.25. The devices were annealed at 80℃ for 5 min after spin-coating. A thin layer of PDINN was subsequently spin-coated from a methanol solution with a concentration of 1.0 mg·ml^{-1} directly onto the active layer. Finally, thermal evaporation was employed to deposit a 120 nm-thick silver (Ag) electrode, resulting in the completion of the devices featuring an active area of 0.06 cm^2, and the testing aperture area was 0.0475 cm^2.

Large-area Device Fabrication

The modules were fabricated with similar device architecture to the small-area OSCs. Glass substrates (5.5 × 5.5 cm^2) are used with predeposited ITO layer. The film stack is laser scribed by a 1064 nm nano-sec beam (2 W) to form isolated cell units. Then Glass substrates with ITO pattern were rinsed with deionized water, acetone and isopropyl alcohol by ultrasonication, sequentially. The gap between the substrate and the blade is 100 μm during the whole

processing. 180 µl of PEDOT: PSS solution was deposited on the substrate by a doctor blade at a blade speed of 3 mm s^{-1} and a substrate temperature of 45 ℃. The thickness of PEDOT: PSS film is 20-30 nm. Then, 90 µl of PM6: L8-BO solution (5.5 mg/ml polymer in toluene, polymer donor: acceptor weight ratio of 1:1.2) was coated on top of PEDOT: PSS layer in ambient with coating speed of 8 mm s^{-1}. The substate temperature was set at 45 ℃. Then, samples were transferred into glove box and annealed at 80 ℃ for 10 min under N_2. As for the electron transport layer, 90 µl of PNDIT-F3N solution (1.5 mg/ml in methanol, 0.3% v/v acetic acid) was subsequently coated atop of active layer at a speed of 5 mm s^{-1} with setting substrate at room temperature. The thickness of PNDIT-F3N film is 10-15 nm. A 532 nm nano-sec laser beam (2 W) is used for P2 scribing to expose the top ITO layer for later series connection. 150 nm Ag electrode is vacuum deposited to finalize the module layer stack. P3 scribing edge isolation are carried out with the same 532 nm nano-sec beam (2 W). The modules are interconnected by 8 subcells with an active area of 4 × 0.478 cm^2 for each subcell. The geometric fill factor (GFF) is 0.956.

Cyclic Voltammetry (CV) Measurement

CV measurement was conducted using a CHI600A electrochemical workstation by utilizing the acetonitrile solution of 0.1 mol/L tetrabutylammoniumhexafluorophosphate (Bu_4NPF_6). The CV curves were recorded versus the potential of the standard calomel electrode (SCE), which was calibrated by the ferrocene-ferrocenium (FC/FC^+) redox couple (4.8 eV below the vacuum level). Subsequently, the calculation of the lowest unoccupied molecular orbital (LUMO) and the highest occupied molecular orbital (HOMO) energy levels was performed using the equation of $E_{LUMO/HOMO} = -e(E_{red/ox}+4.39)$ (eV).

Absorption Measurement

The UV-vis absorption spectra were measured from a U-4100 (HITACHI) UV-vis spectrophotometer.

UPS Measurement

UPS measurement was carried out by Thermo Fisher ESCALAB Xi^+ in an ultrahigh vacuum chamber (in the order of 10^{-10} mbar). A low-intensity UV light (He I line) with excitation energy of 21.22 eV was used, and the bias voltage of 10 V was applied.

Contact Angle Measurement

Contact angles of water and diiodomethane on all films were measured using a contact angle system (DropMeter A-200, MAIST).

The Flory-Huggins Interaction Parameter Calculation

$$\chi = (\sqrt{\gamma_1} - \sqrt{\gamma_2})^2 \quad (1)$$

Nuclear Magnetic Resonance Spectroscopy (NMR) Measurement

All compounds were characterized by ^{1}H NMR (500 MHz, $CDCl_3$) on a Bruker Avance III 500 nuclear magnetic resonance spectroscope at room temperature.

Differential Scanning Calorimetry (DSC) Measurements

DSC measurements were performed on the PerkinElmer Diamond DSC instrument with a heating rate of 10 ºC min^{-1} under nitrogen atmosphere.

***J-V* and EQE Measurement**

The *J-V* measurement was performed via the solar simulator (SS-X50, Enlitech) equipped with AM 1.5G spectra. The intensity was calibrated using the certified reference standard silicon solar cell (KG2) at an irradiance of 100 mW·cm^2. The external quantum efficiency (EQE) data were obtained using the solar-cell spectral-response measurement system (RE-R, Enlitech).

Solar Module Characterization

The *J-V* characteristic curves of modules were recorded via the solar simulator (SS-F5-3A, Enlitech) and AM 1.5G spectra, calibrating the light intensity of the certified standard silicon solar cell (SRC 2020, Enlitech) at 100 mV cm^{-2}. *J-V* scan speed and dwell time are 0.05 V/step and 1 ms, respectively. The *J-V* measurements of modules were performed in a glovebox under N_2 atmosphere with the aperture (16.00 cm^2 full open area, no shade in interconnection area).

Transient Absorption Spectroscopy (TAS) Measurement

To perform femtosecond transient absorption spectroscopy, the fundamental output from Yb:KGW laser (1030 nm, 220 fs Gaussian fit, 100 kHz, Light Conversion Ltd) was separated to two light beam. One beam passed through a NOPA (ORPHEUS-N, Light Conversion Ltd) to produce a certain wavelength for pump beam (here we use 750 nm, <10 $\mu j \cdot cm^{-2}$), while the other was focused onto a YAG plate to generate a white light continuum as probe beam. The pump and probe beams were overlapped on the sample at a small angle (< 10°). The transmitted probe light from sample was collected by a linear CCD array. Then we obtained transient differential transmission signals by equation shown below:

$$\frac{\Delta T}{T} = \frac{T_{\text{pump - on}} - T_{\text{pump - off}}}{T_{\text{pump - off}}} \qquad (2)$$

Space Charge Limited Current (SCLC) Measurement

Hole-only devices were fabricated in a structure of ITO/PEDOT:PSS/Active Layer/M_OO_3/Ag. Electron only devices were fabricated in ITO/ZnO/Active Layer/PDINN/Ag structure. The device characteristics were extracted by modeling the dark current under forwarding bias using the SCLC expression described by the Mott-Gurney law:

$$J = \frac{9}{8}\varepsilon_r \varepsilon_0 \mu \frac{V^2}{L^3} \qquad (3)$$

Here, $\varepsilon_r \approx 3$ is the average dielectric constant of the blend film, ε_0 is the permittivity of the free space, μ is the carrier mobility, L is the thickness of the film and V is the applied voltage.

Grazing Incidence Small-Angle X-ray scattering (GISAXS) characterization

GIWAXS measurements were performed using a Xeuss 2.0 SAXS/WAXS laboratory beamline using a Cu X-ray source (8.05 keV, 1.54 Å) and a Pilatus3R 300K detector. The incidence angle was 0.2°.

Grazing Incidence Wide-Angle X-ray Scattering (GIWAXS) Characterization

GIWAXS measurements were performed at SAXS/WAXS beamline, Australian Synchrotron ANSTO. Samples were prepared on Si substrates using identical blend solutions as those used in devices. The 15.2 keV X-ray beam was incident at a grazing angle of 0.08°-0.12°, selected to maximize the scattering intensity from the samples. The scattered x-rays were detected using a Dectris Pilatus 2M photon counting detector.

Atomic Force Microscope (AFM) Measurement

AFM images were conducted using a VeecoMultiMode atomic force microscopy in the tapping mode. An etched silicon cantilever was utilized, applying a nominal load of approximately 2 nN. The scanning rate for obtaining a 10 μm × 10 μm image size was set to 1.5 Hz, while for a smaller image size of 1 μm × 1 μm, the scanning rate was adjusted to 1.0 Hz.

Supplementary Figures

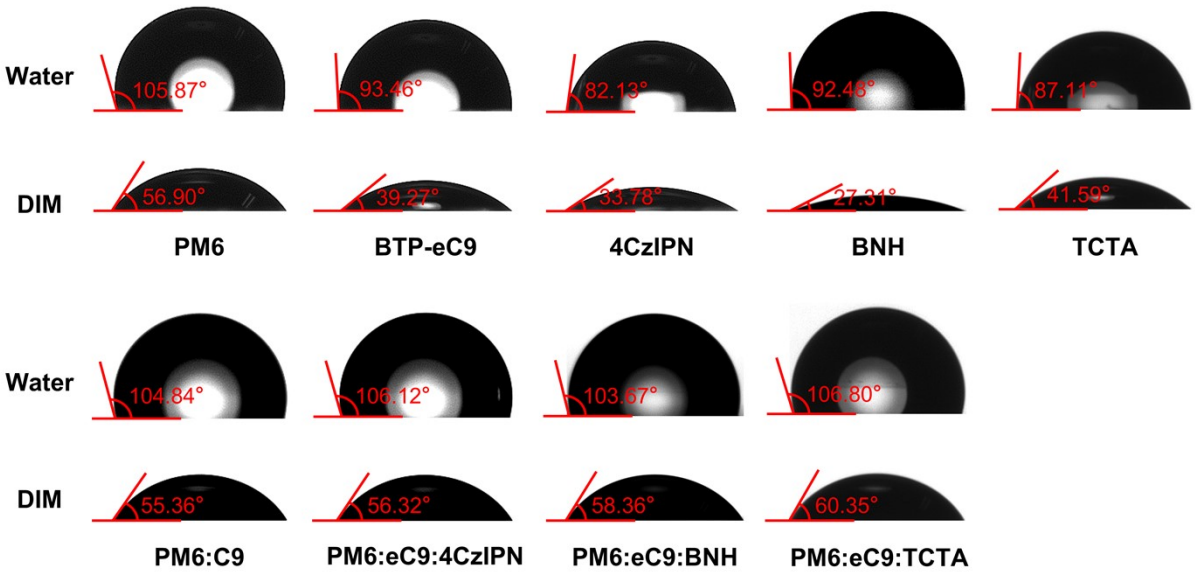

Fig. S1 Contact angle images of various films with water and diiodomethane (DIM).

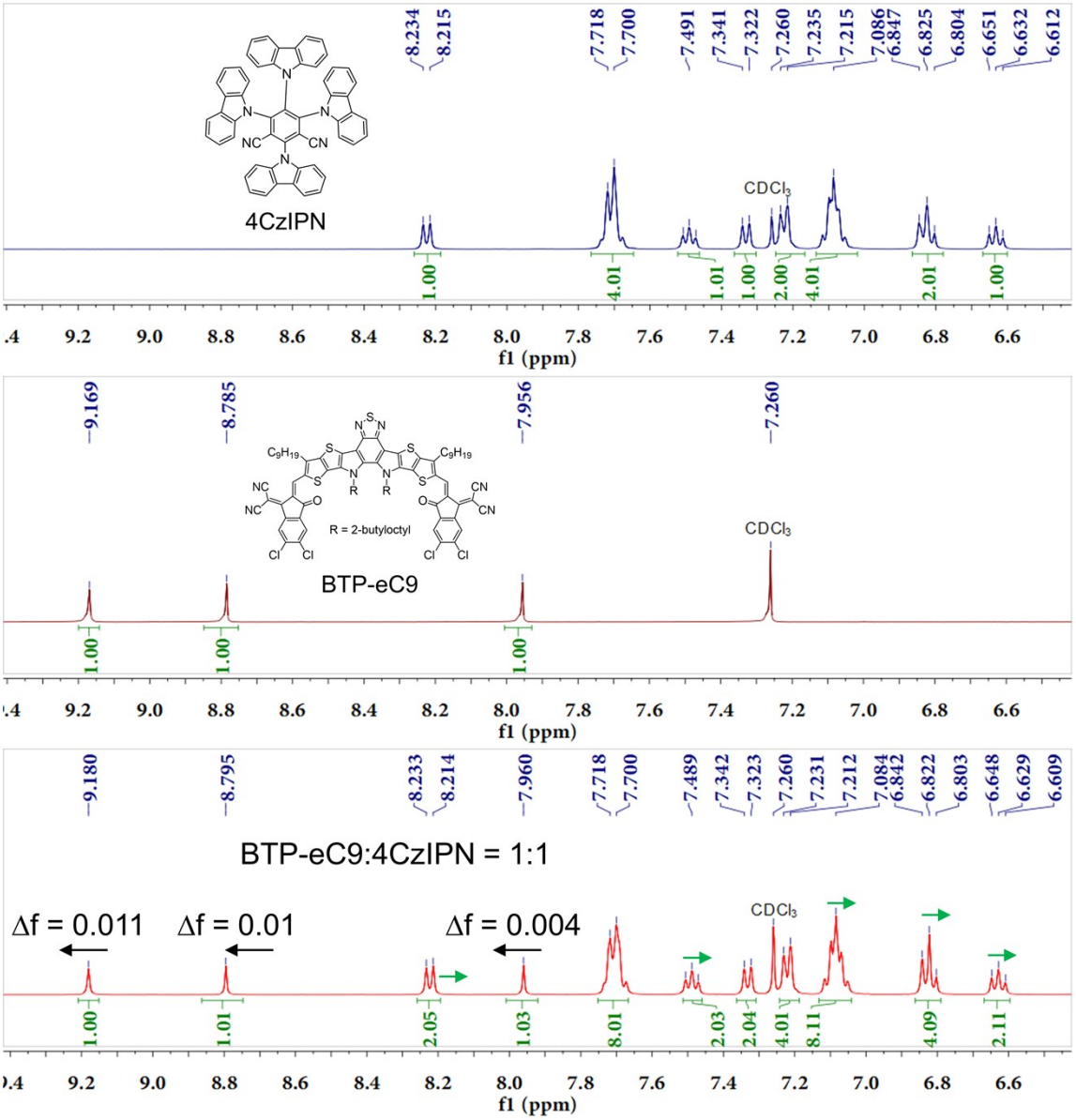

Fig. S2 NMR spectrum of 4CzIPN, BTP-eC9, and their blend.

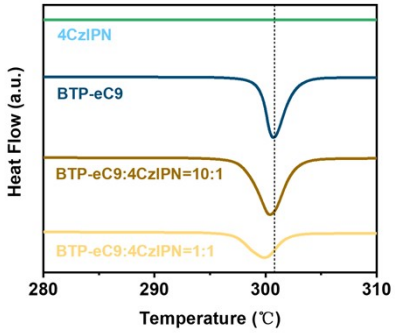

Fig. S3 DSC curves of 4CzIPN, BTP-eC9, and their blend with a heating rate of 10 °C min^{-1} under nitrogen atmosphere.

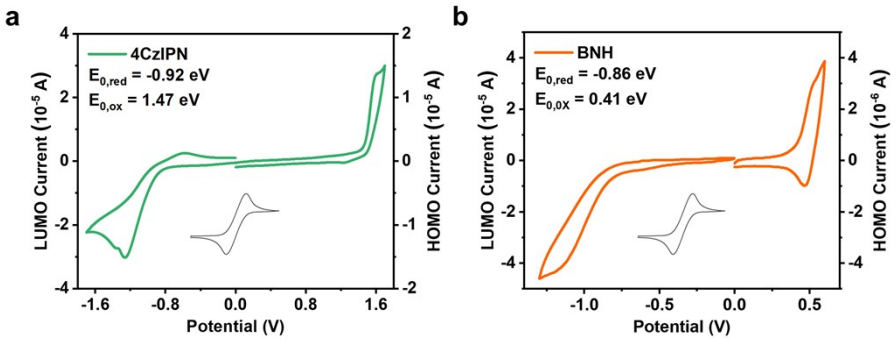

Fig. S4 The Cyclic voltammograms of (a) 4CzIPN and (b) BNH.

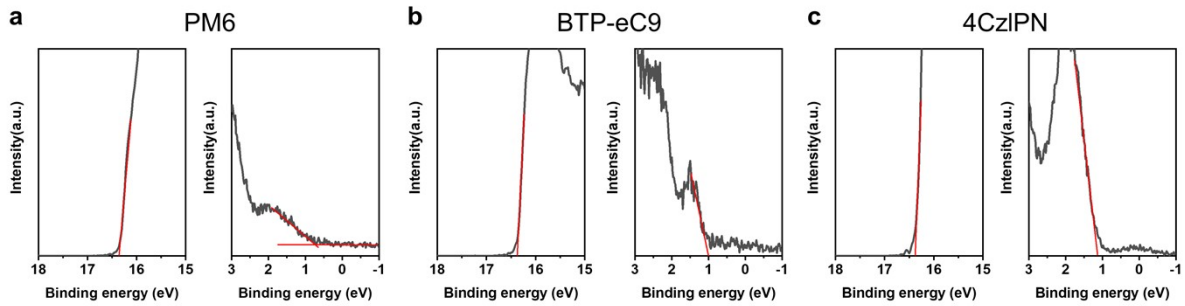

Fig. S5 The UPS profiles of (a) PM6, (b) BTP-eC9, and (c) 4CzIPN.

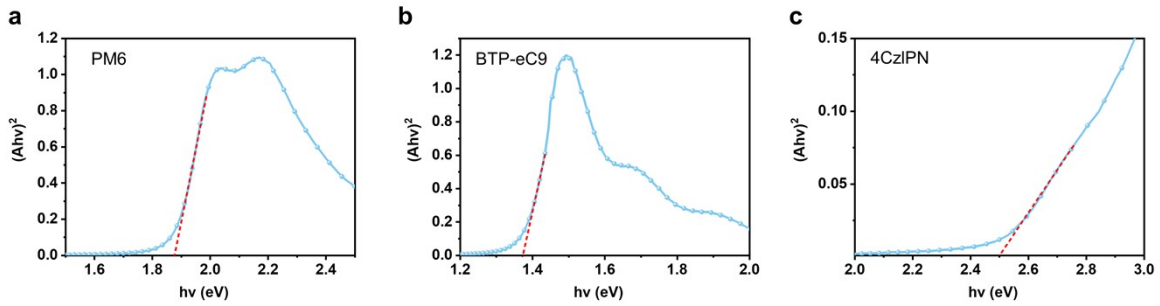

Fig. S6 Method of band gap energy (E_g) determination from the Tauc plot. The linear part of the plot is extrapolated to the x-axis.

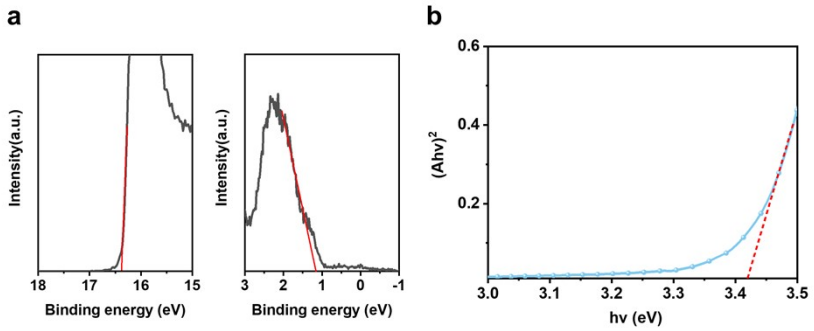

Fig. S7 (a) The UPS profiles of TCTA. (b) Method of band gap energy (E_g) determination from the Tauc plot. The linear part of the plot is extrapolated to the x-axis.

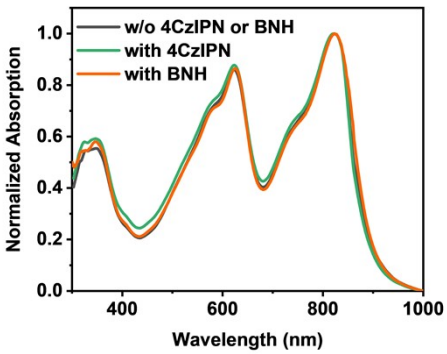

Fig. S8 Normalized UV-vis spectra of blend films (the ratio of TADF:BTP-eC9 is 0.5%).

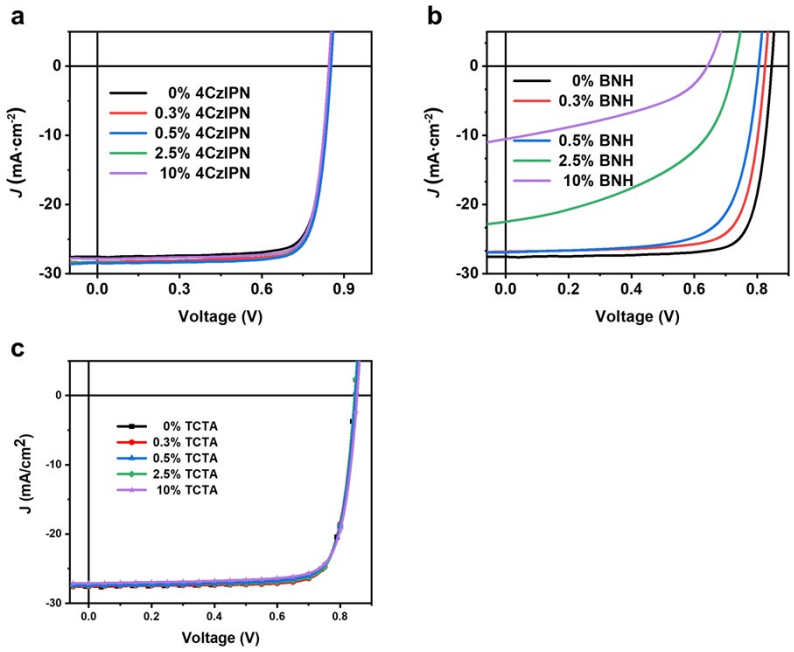

Fig. S9 *J-V* characteristics of devices with different contents of (a) 4CzIPN, (b) BNH, and (c) TCTA.

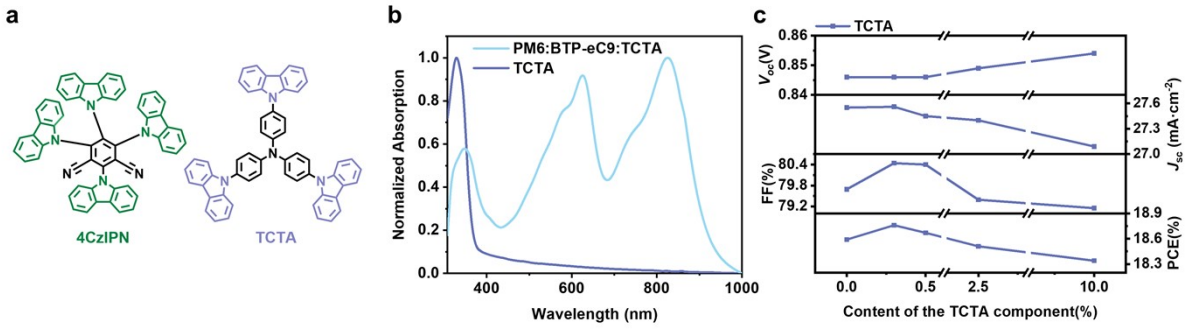

Fig. S10 (a) Chemical structures of 4CzIPN and TCTA. (b) Normalized UV-vis spectra of TCTA and PM6:BTP-eC9:TCTA. (c) *J*-*V* characteristics of optimized devices with TCTA.

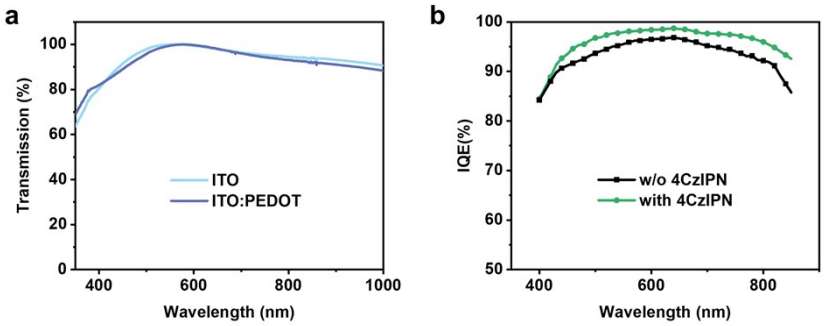

Fig. S11 (a) Transmission curves of ITO, and ITO/PEDOT:PSS. (b) IQE curves of the devices with and without 4CzIPN.

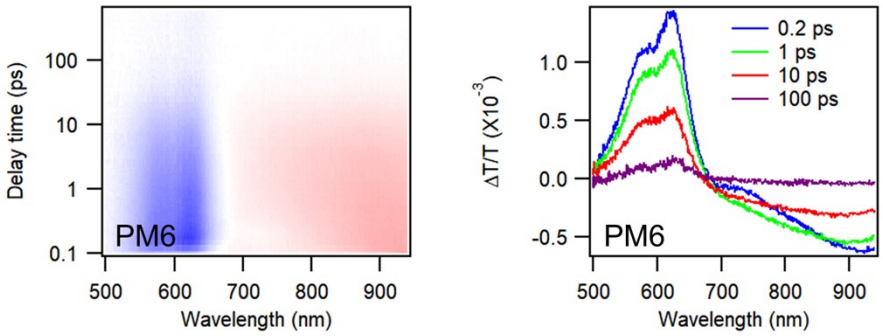

Fig. S12 TA spectra of the PM6 neat film at different delay times.

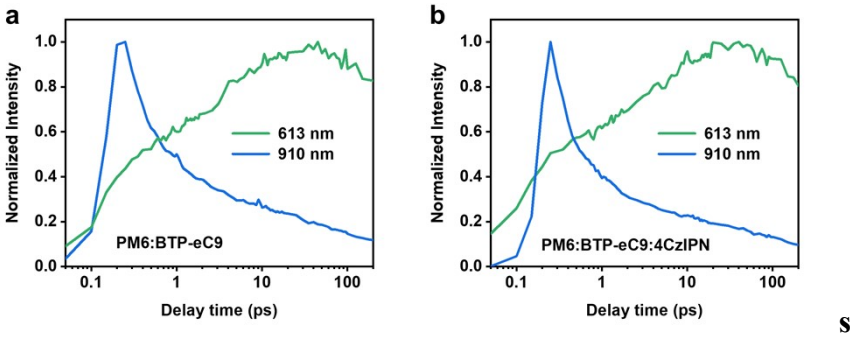

s

Fig. S13 TA traces of blend films with and without 4CzIPN, probed at 613 and 910 nm, respectively.

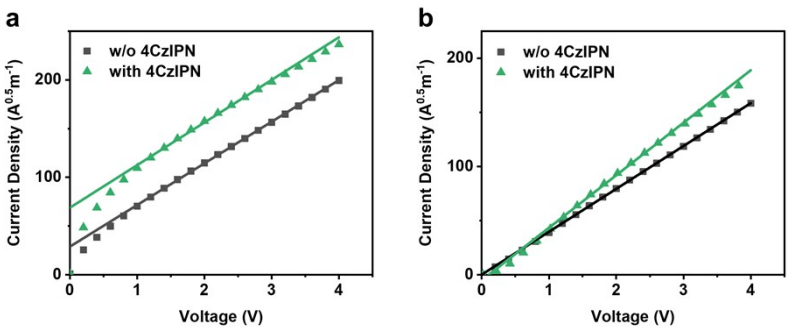

Fig. S14 SCLC curves of (a) hole-only and (b) electron-only devices.

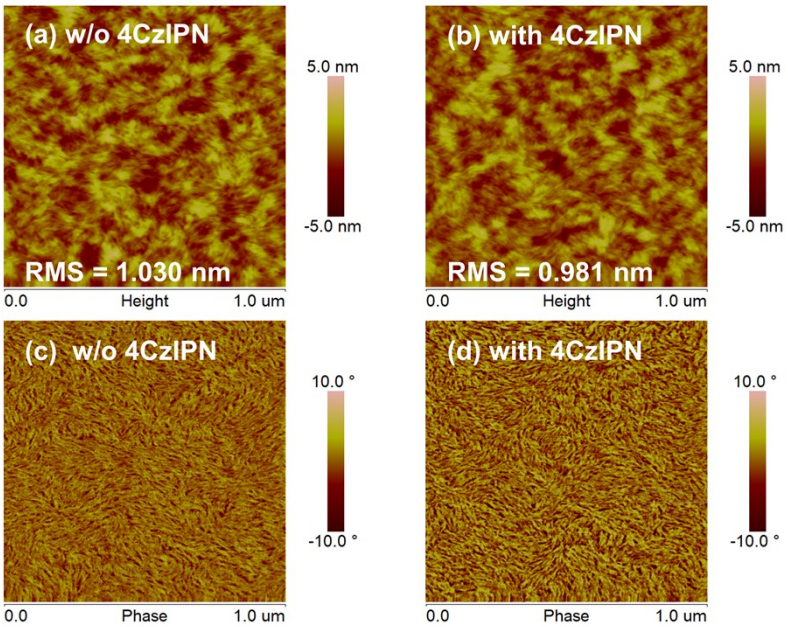

Fig. S15 AFM height images for blend films (a) without 4CzIPN and (b) with 4CzIPN. AFM phase images for blend films (c) without 4CzIPN and (d) with 4CzIPN.

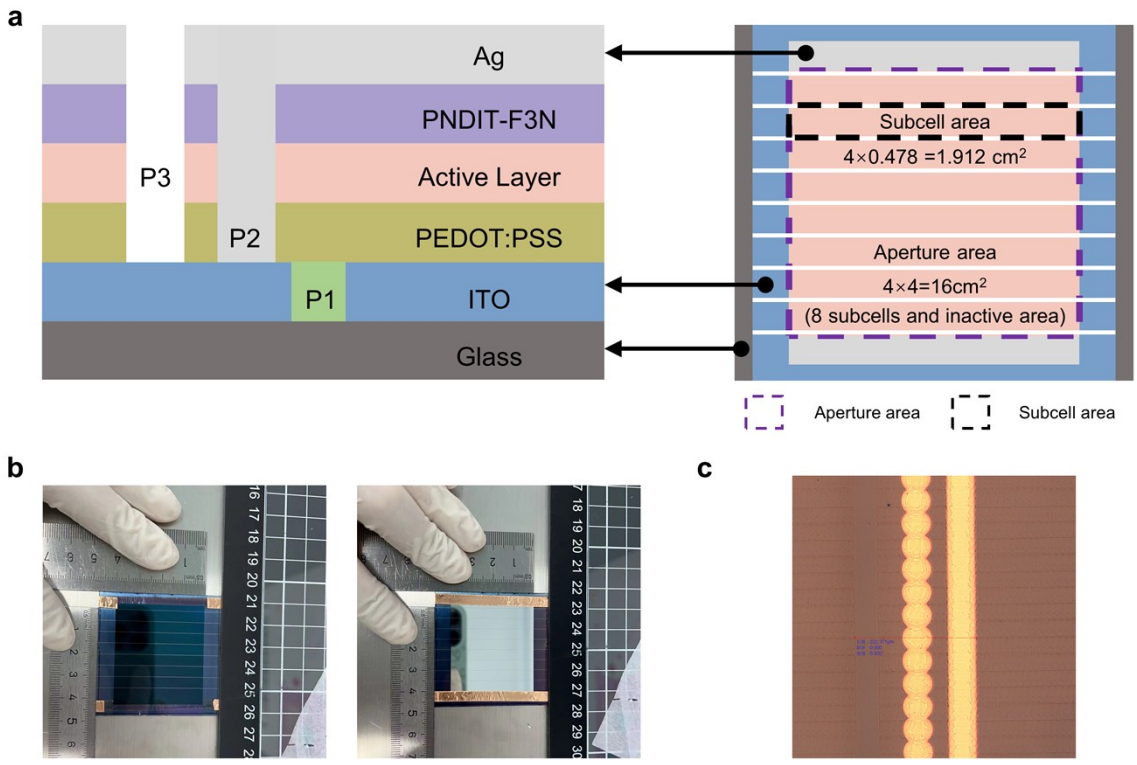

Fig. S16 (a) Schematic illustration of organic solar module. (b) Photo of the organic solar module with the designated aperture area (4×4=16 cm^2). (c) Optical microscope observation of the P1-P2-P3 laser line patterning.

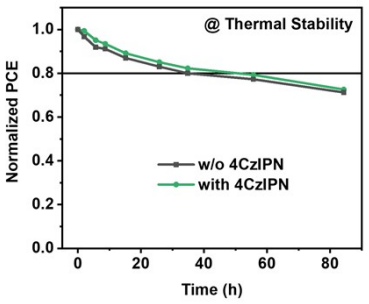

Fig. S17 The thermal stability measurements of devices with and without 4CzIPN by continuous heating the unencapsulated devices at 85 ℃ in glove box.

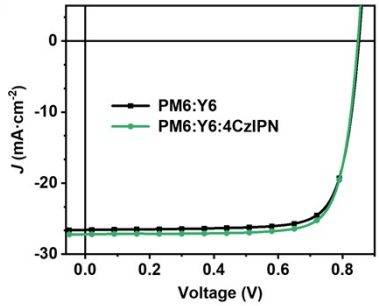

Fig. S18 *J-V* characteristics of optimized devices based on PM6:Y6 and PM6:Y6:4CzIPN.

Supplementary Tables

Table S1. Contact angle of different films with water and diiodomethane, and the calculated surface energy.

Name	Water/°	Diiodomethane/°	Surface Energy /(mN/m)
PM6	105.87	56.90	31.75
BTP-eC9	93.46	39.27	40.48
4CzIPN	82.13	33.78	42.67
BNH	92.48	27.31	46.34
TCTA	87.11	41.59	38.80
PM6: BTP-eC9	104.84	55.36	32.58
PM6:eC9:4CzIPN	106.12	56.32	31.21
PM6:eC9:BNH	103.67	58.36	30.29
PM6:eC9:TCTA	106.80	60.35	29.56

Table S2. The Flory-Huggins interaction parameters between different components.

A1	A2	F-H Interaction Parameter
BTP-eC9	PM6	0.530
BTP-eC9	4CzIPN	0.029
BTP-eC9	BNH	0.198
BTP-eC9	TCTA	0.018
PM6	4CzIPN	0.806
PM6	BNH	1.375
PM6	TCTA	0.353

Table S3. Summarized surface energy level parameters of PM6, BTP-eC9, 4CzIPN, BNH, and TCTA

Materials	$HOMO/LUMO_{CV}$ (eV)	$E_{cut\text{-}off}$ (eV)	E_{onset} (eV)	$HOMO_{ups}$ (eV)	E_g^{opt} (eV)	$LUMO_{opt}$ (eV)
PM6	-5.50/-3.61	16.36	0.76	5.62	1.87	3.75
BTP-eC9	-5.65/-4.10	16.38	1.00	5.84	1.39	4.45
4CzIPN	-5.86/-3.47	16.38	1.12	5.96	2.50	3.46
TCTA	-	16.38	1.14	5.98	3.41	2.57

Active Layer	4CzIPN:C9 (%)	V_{OC} [V]	J_{SC} [mA·cm^{-2}]	FF [%]	PCE [%]
PM6:BTP-eC9: 4CzIPN	0	0.846 (0.847±0.002)	27.55 (27.42±0.15)	79.69 (79.59±0.25)	18.59 (18.43±0.09)
	0.3	0.847 (0.848±0.003)	28.28 (28.13±0.19)	80.02 (79.86±0.31)	19.13 (19.08±0.04)
	0.5	0.852 (0.851±0.003)	28.44 (28.34±0.22)	79.89 (79.83±0.43)	19.40 (19.28±0.07)
	2.5	0.848 (0.849±0.004)	28.36 (28.13±0.26)	80.21 (79.96±0.53)	19.33 (19.11±0.17)
	10	0.844 (0.847±0.002)	27.80 (27.73±0.21)	80.41 (79.74±0.45)	18.97 (18.83±0.11)

Table S4. The devices photovoltaic parameters with different contents of the 4CzIPN.

Table S5. The devices photovoltaic parameters with different contents of the additive BNH.

Active Layer	BNH:C9 (%)	V_{OC} [V]	J_{SC} [mA·cm^{-2}]	FF [%]	PCE [%]
PM6:BTP-eC9: BNH	0	0.846 (0.847±0.002)	27.55 (27.42±0.15)	79.69 (79.59±0.25)	18.59 (18.43±0.09)
	0.3	0.825 (0.823±0.002)	26.80 (26.81±0.27)	76.45 (75.22±0.92)	16.91 (16.59±0.21)
	0.5	0.805 (0.801±0.003)	26.90 (26.84±0.11)	70.91 (68.93±1.20)	15.36 (14.83±0.32)
	2.5	0.726 (0.730±0.003)	22.48 (22.14±0.19)	47.41 (47.09±0.27)	7.74 (7.62±0.10)
	10	0.642 (0.642±0.003)	10.54 (9.82±0.39)	40.08 (39.78±0.31)	2.71 (2.51±0.12)

Table S6. The devices photovoltaic parameters with different contents of the additive TCTA.

Active Layer	TCTA:C9 (%)	V_{OC} [V]	J_{SC} [mA·cm^{-2}]	FF [%]	PCE [%]
PM6:BTP-eC9: TCTA	0	0.846 (0.847±0.002)	27.55 (27.42±0.15)	79.69 (79.59±0.25)	18.59 (18.43±0.09)
	0.3	0.846 (0.848±0.001)	27.56 (27.50±0.14)	80.44 (79.85±0.29)	18.76 (18.61±0.11)
	0.5	0.846 (0.847±0.001)	27.45 (27.05±0.21)	80.40 (80.30±0.15)	18.67 (18.40±0.15)
	2.5	0.849 (0.847±0.001)	27.40 (27.23±0.16)	79.39 (79.22±0.49)	18.51 (18.31±0.14)
	10	0.854 (0.852±0.002)	27.09 (26.90±0.11)	79.15 (79.04±0.20)	18.34 (18.15±0.08)

Table S7. Detailed kinetic fitting parameters of hole transfer for optimal blend films.

Active Layer	A_1 (%)	τ_1 (ps)	A_2 (%)	τ_2 (ps)
with 4CzIPN	60.2	0.133±0.011	41.3	4.949±0.284
without 4CzIPN	62.5	0.147±0.009	43.1	4.303±0.203

The hole transfer kinetics of blend films can be fitted by a biexponential function: $i = A_1\exp(-t/\tau_1) + A_2\exp(-t/\tau_2)$, with fast and slow lifetimes of τ_1 and τ_2 and prefactors of A_1 and A_2.

Table S8. The calculated GIWAXS parameters of the various films in IP.

In-Plane (100)	location/$Å^{-1}$	d-spacing/Å	FWHM	CCL/Å
C9	0.398	15.773	-	-
w/o 4CzIPN	0.295	21.294	0.067	84.75
with 4CzIPN	0.302	20.787	0.070	80.65

Table S9. The calculated GIWAXS parameters of the various films in OOP.

Out-Of-Plane (010)	location/$Å^{-1}$	d-spacing/Å	FWHM	CCL/Å
C9	1.763	3.565	-	-
4CzIPN	1.554	4.043	-	-
w/o 4CzIPN	1.749	3.592	0.176	32.04
with 4CzIPN	1.761	3.569	0.193	29.34

Table S10. The detailed parameters of Solar module.

Solid Additive	V_{OC} [V]	I_{SC} [mA]	FF [%]	PCE[a)] [%]	PCE[b)] [%]
w/o	7.01 (7.01±0.04)	45.36 (44.80±1.14)	69.62 (69.49±1.65)	13.82 (13.64±0.17)	14.46 (14.26±0.17)
4CzIPN	7.01 (7.03±0.06)	43.96 (44.50±0.74)	74.68 (72.90±1.39)	14.39 (13.86±0.12)	15.06 (14.92±0.12)

[a)]PCE with respect to the aperture area of 16.000 cm^2; [b)]PCE with respect to the active area of 15.296 cm^2; The numbers in parentheses represent the average parameters for at least 10 modules.

Table S11. The detailed parameters of OPV devices w/o and with 4CzIPN.

Active Layer		V_{OC} [V]	J_{SC} [mA·cm^{-2}]	FF [%]	PCE [%]
PM6:L8-BO	w/o 4CzIPN	0.879 (0.880±0.002)	26.22 (26.09±0.27)	80.15 (79.97±0.54)	18.52 (18.38±0.07)
	with 4CzIPN	0.886 (0.883±0.003)	26.90 (26.86±0.04)	80.55 (80.51±0.14)	19.20 (19.10±0.05)
PM6:Y6	w/o 4CzIPN	0.851 (0.852±0.001)	26.58 (26.63±0.20)	78.07 (76.95±0.71)	17.69 (17.48±0.24)
	with 4CzIPN	0.848 (0.851±0.002)	27.22 (27.02±0.27)	78.75 (78.54±1.03)	18.20 (18.07±0.08)